



HAL
open science

CBOC performances using software receiver

Géraldine Artaud, Lionel Ries, J Dantepal, Jean-Luc Issler, T Grelier,
Antoine Delatour, Olivier Julien, Christophe Macabiau

► **To cite this version:**

Géraldine Artaud, Lionel Ries, J Dantepal, Jean-Luc Issler, T Grelier, et al.. CBOC performances using software receiver. GNSS Signal 2007, 2nd Workshop on GNSS Signals and Signals Processing, Apr 2007, Noordwijk, Netherlands. hal-01021986

HAL Id: hal-01021986

<https://hal-enac.archives-ouvertes.fr/hal-01021986>

Submitted on 20 Nov 2014

HAL is a multi-disciplinary open access archive for the deposit and dissemination of scientific research documents, whether they are published or not. The documents may come from teaching and research institutions in France or abroad, or from public or private research centers.

L'archive ouverte pluridisciplinaire **HAL**, est destinée au dépôt et à la diffusion de documents scientifiques de niveau recherche, publiés ou non, émanant des établissements d'enseignement et de recherche français ou étrangers, des laboratoires publics ou privés.

CBOC PERFORMANCES USING SOFTWARE RECEIVER

GNSS Signal 2007, 24 - 25 April 2007 at ESTEC, Noordwijk, the Netherlands

G. Artaud⁽¹⁾, L. Ries⁽¹⁾, J. Dantepal⁽¹⁾, JL. Issler⁽¹⁾, T. Grelier⁽¹⁾, A. Delatour⁽¹⁾, O. Julien⁽²⁾, C. Macabiau⁽²⁾

⁽¹⁾CNES

18, avenue Edouard Belin
31401 Toulouse cedex 9, France
Email: geraldine.artaud@cnes.fr

⁽²⁾ENAC

7 avenue Edouard Belin
31055 Toulouse cedex 4, France

INTRODUCTION

MBOC(6,1,1/11) [1] has been identified as a promising modulation for the optimisation of Galileo E1 OS and GPSIII L1C. The corresponding power spectral density is the combination of BOC(1,1) and BOC(6,1) PSD and a number of modulations lead to the targeted power spectral density. One of the solution, that seems to be the favourite candidate for Galileo, is the Composite BOC (CBOC). It adds linearly the BOC(1,1) and BOC(6,1) waveform creating a multi-level waveform. Several more or less complex receiver's architecture can be used to track CBOC signals offering different performances in various degraded environment.

The theoretical performances of CBOC have already been presented in several articles. The aim of this article is to assess CBOC performances for a number of receiver architectures implemented in a software receiver. The first step consist in generating CBOC signal using a software generator and it was considered as a second step to generate CBOC signal using a RF signal generator.

CBOC SIGNAL

Signal Definition

The power spectral density of MBOC(6,1,1/11) is:

$$G_{signal} = \frac{10}{11} G_{BOC(1,1)}(f) + \frac{1}{11} G_{BOC(6,1)}(f)$$

where $G_{BOC(m,n)}(f)$ is the unit-power PSD of a sine phased BOC spreading modulation.

In order to comply with the optimized spectrum, a number of implementations are possible [2]. Two implementations of CBOC using a 50%/50% power split between data and pilot components are considered. The first implementation uses both CBOC on data and pilot channel, the second uses only CBOC on pilot channel and BOC(1,1) on data channel. By representing only the OS signal, the two implementations can be described by the following equations:

$$s_1(t) = A_1 \left[\begin{array}{l} \text{Data} \cdot C_{\text{Data}} \cdot \{aBOC(1,1) + bBOC(6,1)\} \\ + C_{\text{Pilot}} \cdot \{aBOC(1,1) - bBOC(6,1)\} \end{array} \right] \quad (1)$$

$$s_2(t) = A_2 \left[\begin{array}{l} k_1 \text{Data} \cdot C_{\text{Data}} \cdot BOC(1,1) \\ + C_{\text{Pilot}} \cdot \{aBOC(1,1) - (-1)^n bBOC(6,1)\} \end{array} \right] \quad (2)$$

The following notation can be used:

$$\begin{aligned} CBOC(6,1,p,-')(t) &= C(t) \{aBOC(1,1)(t) - bBOC(6,1)(t)\} \\ CBOC(6,1,p,+')(t) &= C(t) \{aBOC(1,1)(t) + bBOC(6,1)(t)\} \\ CBOC(6,1,p,+/-')(t) &= \begin{cases} C(t) \{aBOC(1,1)(t) + bBOC(6,1)(t)\} & \text{even chips} \\ C(t) \{aBOC(1,1)(t) - bBOC(6,1)(t)\} & \text{odd chips} \end{cases} \end{aligned} \quad (3)$$

where $p = \frac{b^2}{a^2 + b^2}$

For signal using CBOC both on pilot and data channel, $a = \sqrt{\frac{10}{11}}$ and $b = \sqrt{\frac{1}{11}}$. On the data Channel BOC(6,1) is added to BOC(1,1): CBOC(6,1,1/11,'+'), On the pilot channel, it is subtracted: CBOC(6,1,1/11,'-').

For signal using CBOC only on pilot channel $a = \sqrt{\frac{9}{22}}$ and $b = \sqrt{\frac{1}{11}}$, and BOC(6,1) is alternated in sign: CBOC(6,1,2/11,'+/-').

Receivers Architecture

It is proposed to evaluate in this article three types of receivers: a baseline Galileo receiver implementing only the BOC(1,1) subcarrier; a receiver based on the architecture presented by Olivier Julien [3] using either a pure BOC(1,1) or a pure BOC(6,1) subcarrier in the correlation process and a traditional CBOC receiver.

The impact of the optimized CBOC waveform on a receiver design to process BOC(1,1) is evaluated using a Galileo baseline receiver. Two cases are studied: a BOC(1,1) receiver with a narrow one sided precorrelation bandwidth of 2MHz, and a BOC(1,1) receiver with wide bandwidths similar to those used by CBOC receivers.

The second type of receiver performs 1-bit processing of MBOC using one correlator. Its structure has been presented in detail in [3], it enables tracking of CBOC signal as well as TMBOC signal. A local replica similar to TMBOC (named TM61) is generated: the receiver uses a pure BOC(1,1) for the prompt correlation and a pure BOC(6,1) for the early-late correlation. The architecture is presented in Fig 1.

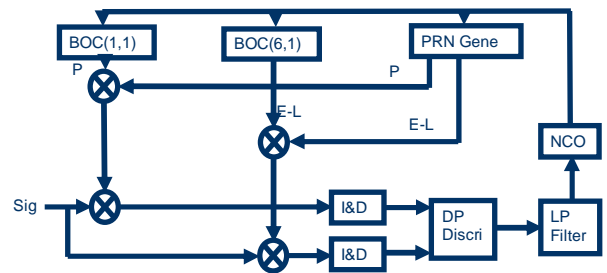


Fig. 1: TM61 Tracking Architecture

The third type of receiver is a pure CBOC receiver, optimized to track the incoming CBOC signal.

Theoretical CBOC tracking performances

Assuming a DP discriminator and, the theoretical tracking error variance due to thermal noise is given by [3][4]:

$$\sigma_{DP}^2 = \left(\frac{B_L(1-0.5B_L T_I)(\tilde{R}_{Lel}(0) - \tilde{R}_{Lel}(d))}{\frac{P}{2N_0} \left(\left. \frac{d\tilde{R}_{Ccl}(x)}{dx} \right|_{x=\frac{d}{2}} \right)^2} \times \left(1 + \frac{\tilde{R}_{Lp}(0)}{\frac{P_r T_I}{N_0} \tilde{R}_{Cp}^2(0)} \right) \right) \quad (4)$$

where B_L is the DLL loop bandwidth,

T_I is the coherent integration time,

d is the early-late spacing,

P_r is the incoming useful signal power (in the data or pilot channel),

N_0 is the thermal noise PSD level,

\tilde{R}_{Lx} is the filtered correlator output noise correlation function, it involves the local replica correlation function for prompt correlation ($x=p$) and early-late correlation ($x=el$), and

\tilde{R}_{Cx} is the filtered correlation function of the incoming signal with the local replica for prompt correlation ($x=p$) and early-late correlation ($x=el$).

Assuming that the front-end filter has a unity gain within $\pm B$ Hz, and is null elsewhere, it can be shown [4] that:

$$\tilde{R}_{LeI}(0) - \tilde{R}_{LeI}(d) = \int_{-B}^B G_{LeI}(f) \sin^2(\pi f d) df \quad (5)$$

$$\left. \frac{d\tilde{R}_{CeI}(x)}{dx} \right|_{x=\frac{d}{2}} = 2\pi \int_{-B}^B f G_{CeI}(f) \sin(\pi f d) df \quad (6)$$

$$\tilde{R}_{Lp}(0) = \int_{-B}^B G_{Lp}(f) df \quad (7)$$

$$\tilde{R}_{Cp}(0) = \int_{-B}^B G_{Cp}(f) df \quad (8)$$

$$\sigma_{DP}^2 = \left(\frac{B_L(1 - 0.5B_L T_i) \left(\int_{-B}^B G_{LeI}(f) \sin^2(\pi f d) df \right)}{\frac{P}{2N_0} \left(2\pi \int_{-B}^B f G_{CeI}(f) \sin(\pi f d) df \right)^2} \times \left(1 + \frac{\int_{-B}^B G_{Lp}(f) df}{\frac{P_r T_i}{N_0} \left(\int_{-B}^B G_{Cp}(f) df \right)^2} \right) \right)$$

Depending on the CBOC signal and the implemented receiver architecture, the power spectral densities have the following expressions:

Let's introduce the function $\{s\}$:

$$\{s\} = \begin{cases} +1 & \text{for CBOC}(6,1, p, '+') \\ -1 & \text{for CBOC}(6,1, p, '-') \\ 0 & \text{for CBOC}(6,1, p, '+/-') \end{cases} \quad (9)$$

- Pure CBOC receiver:

$$G_{LeI}(f) = G_{Lp}(f) = G_{CeI}(f) = G_{Cp}(f) = a^2 G_{BOC(1,1)}(f) + b^2 G_{BOC(6,1)}(f) + \{s\} 2ab G_{BOC(1,1)/BOC(6,1)}(f) \quad (10)$$

- BOC(1,1) receiver:

$$G_{LeI}(f) = G_{Lp}(f) = G_{BOC(1,1)}(f)$$

$$G_{CeI}(f) = G_{Cp}(f) = TF(CBOC) \times TF^*(BOC(1,1)) = a G_{BOC(1,1)}(f) + \{s\} b G_{BOC(1,1)/BOC(6,1)}(f) \quad (11)$$

- TM61 receiver:

$$G_{LeI}(f) = G_{BOC(6,1)}(f)$$

$$G_{Lp}(f) = G_{BOC(1,1)}(f)$$

$$G_{Cp}(f) = TF(CBOC) \times TF^*(BOC(1,1)) = a G_{BOC(1,1)}(f) + \{s\} b G_{BOC(1,1)/BOC(6,1)}(f)$$

$$G_{CeI}(f) = TF(CBOC) \times TF^*(BOC(6,1)) = b G_{BOC(6,1)}(f) + \{s\} a G_{BOC(1,1)/BOC(6,1)}(f) \quad (12)$$

The normalized PSD of a sinus BOC(m,n) is given by [5]:

$$G_{BOC(m,n)}(f) = f_c \left(\frac{\sin\left(\frac{\pi f}{f_c}\right) \sin\left(\frac{\pi f}{K f_c}\right)}{\pi f \cos\left(\frac{\pi f}{K f_c}\right)} \right)^2 \quad \text{with } K=2m/n \quad (13)$$

The normalized PSD resulting from the cross correlation is given by the product of the Fourier transform of BOC(n,n) with the conjugate Fourier transform of BOC(m,n) :

$$G_{BOC(n,n)/BOC(m,n)}(f) = f_c \left(\frac{\sin\left(\frac{\pi f}{f_c}\right)}{\pi f} \right)^2 \left(\frac{\sin\left(\frac{\pi f}{2f_c}\right) \sin\left(\frac{\pi f}{K f_c}\right)}{\cos\left(\frac{\pi f}{2f_c}\right) \cos\left(\frac{\pi f}{K f_c}\right)} \right) \quad \text{with } K=2m/n. \quad (14)$$

The theoretical expressions calculated above were compared to the simulations results. They provide the same tendencies in terms of relative performances.

JUZZLE SOFTWARE RECEIVER

Series of simulations have been held using the Juzzle software receiver developed by CNES. It has been configured to generate the two CBOC signal configurations (CBOC on data and pilot component and CBOC on pilot component only) and some development have been done in order to implement the new receiver's architectures. The Juzzle SW receiver is a "bit-true" simulator, two minutes of signal has been generated for each simulation in standard and degraded environments with various front end filters.

The Juzzle SW receiver is based on the open source tool Juzzle (www.juzzle.org), it is written in C ANSI and is multiplatform. Its architecture is organized around libraries and functional blocks. They contain the basic functionalities that have been identified by exploiting the commonalities between the GNSS signals. The receiver can process simulated signal as well as real IF samples recorded by RF equipment. The different modules of the simulator include the receiver performing signal acquisition and tracking; and signal generation, propagation channel and RF stage emulation in order to simulate signals, and binary file reader for post processing of recorded signals

The signal generator provides a highly configurable satellite model, covering various signal configurations of Galileo and GPS IIF. Up to four channels can be multiplexed by the mapping module. Each channel is composed of a data generator, PRN generator and a subcarrier modulator generating BOC(m,n) and BCS waveforms.

The Galileo E1 civil signals on data and pilot channels are generated using two 4092 chip long spreading at 1.023MHz and secondary codes. The CBOC subcarriers are produced using time-dependent look-up tables.

The propagation module produces basic propagation phenomena and is responsible for multipath generation.

The RF stage is also modelled (Rx Filter, AGC, A/D converter). The front-end filters are Root Raised Cosine filters with a roll-off factor of 0,1.

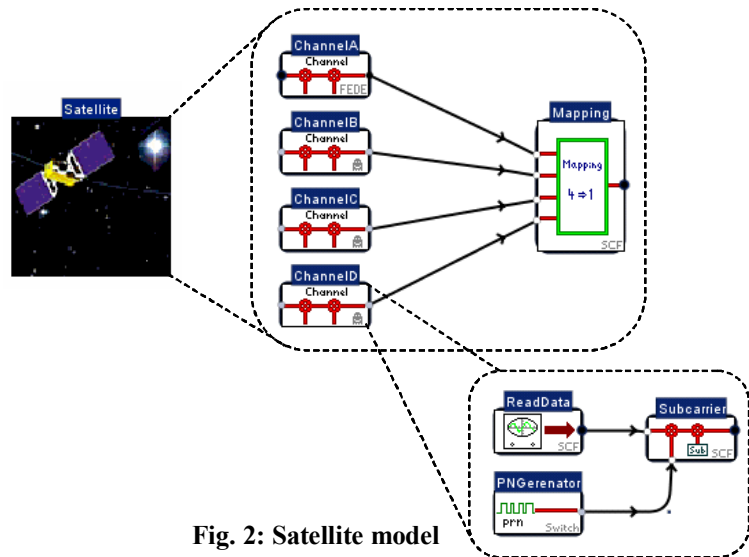


Fig. 2: Satellite model

The SW receiver comprises acquisition and tracking modules and a controller performing autonomous transition between acquisition, tracking and bit synchronisation leading to the extraction of the navigation message. For the purposes of this article only the tracking module is used. It consists of traditional DLL/FLL/FPLL/PLL tracking loops (Fig 3). The tracking architecture is common for all types of received signals; only the correlators and the discriminator normalisation differs between the 3 receiver's architectures.

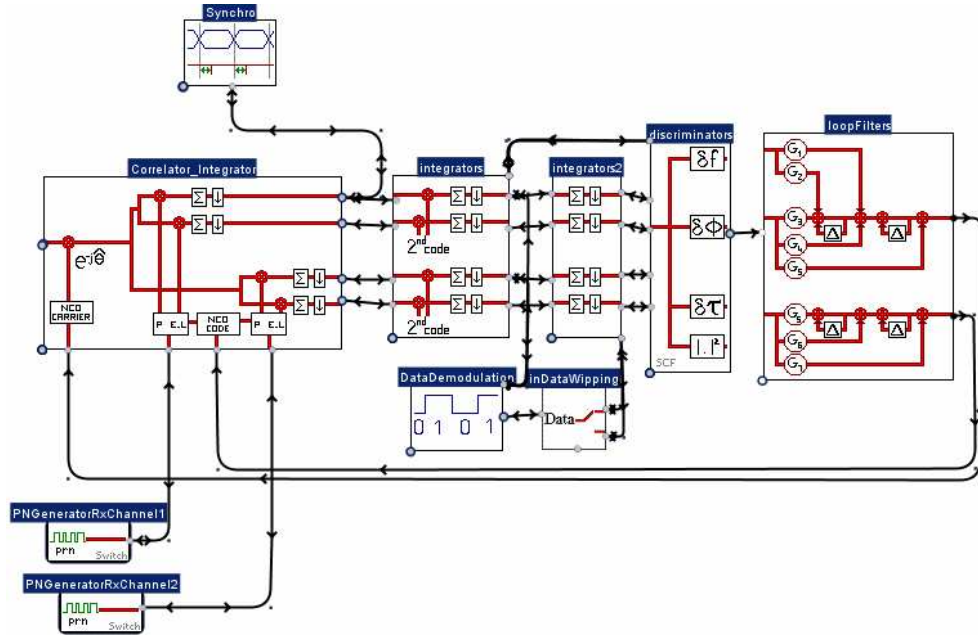


Fig. 3: Tracking architecture

The receiver implements for the DLL a classical Dot-Product discriminator, normalized by the power of the signal. Adjustment of the normalisation shall be performed in order to have a unity gain discriminator at the origin. Without adjustment the dotproduct discriminator can be written as:

$$DDP_N = \frac{I_p(I_e - I_l) + Q_p(Q_e - Q_l)}{I_p^2 + Q_p^2} = \frac{R_{el}\left(\varepsilon - \frac{\delta}{2}\right) - R_{el}\left(\varepsilon + \frac{\delta}{2}\right)}{R_p(\varepsilon)} \quad (15)$$

where R_{el} is the correlation function for early and late correlators and R_p is the correlation function for prompt correlators.

Assuming an infinite front-end filter, and a chip spacing value inferior to the one-sided width of the spreading symbol's main peak, the autocorrelation function of BOC(m,n) signals can be expressed as [4]: $R(\varepsilon) = 1 - \alpha|\varepsilon|$, with

$\alpha = \frac{4m}{n} - 1$. The cross correlation between BOC(n,n) and BOC(m,n) assuming $\left|\frac{\delta'}{2}\right| < \frac{1}{K}$ where $K = \frac{2m}{n}$ can be

modelled as: $R_{BOC(n,n)/BOC(m,n)}(\varepsilon) = |\varepsilon|$.

The dot product discriminator for the three types of receivers shall consequently be normalised to ensure unity gain at the origin by:

- For pure CBOC receiver:

$$CBOC(m, n, '-'): \frac{a^2 + b^2}{2(a^2\alpha_{BOC(1,1)} + b^2\alpha_{BOC(6,1)} - 2ab)}$$

$$CBOC(m, n, '+'): \frac{a^2 + b^2}{2(a^2\alpha_{BOC(1,1)} + b^2\alpha_{BOC(6,1)} + 2ab)} \quad (16)$$

$$CBOC(m, n, '+/-'): \frac{a^2 + b^2}{2(a^2\alpha_{BOC(1,1)} + b^2\alpha_{BOC(6,1)})}$$

- For BOC(1;1) receiver:

$$CBOC(m, n, '-') / BOC(1,1): \frac{a}{2(a\alpha_{BOC(1,1)} + b\alpha_{BOC(6,1)})}$$

$$CBOC(m, n, '+') / BOC(1,1): \frac{a}{2(a\alpha_{BOC(1,1)} - b\alpha_{BOC(6,1)})} \quad (17)$$

$$CBOC(m, n, '+/-') / BOC(1,1): \frac{1}{2(\alpha_{BOC(1,1)})}$$

$$\begin{aligned}
CBOC(m, n, '-'): & \frac{a}{2(b\alpha_{BOC(6,1)} + a)} \\
\bullet \text{ For TM61 receiver: } CBOC(m, n, '+'): & \frac{a}{2(b\alpha_{BOC(6,1)} - a)} \\
CBOC(m, n, '+/-'): & \frac{a}{2(b\alpha_{BOC(6,1)})}
\end{aligned} \tag{18}$$

SIMULATIONS

Series of simulations have been held using the software receiver with different configurations. The two types of CBOC signal are transmitted and are received in the same conditions by the three receivers. Throughout this chapter, the results are given in function of the signal to noise ratio of the incoming CBOC signal.

A first series of simulations have been performed in presence of thermal noise only, and a second series in presence of thermal noise and multipath.

The chosen multipath scenario corresponds to an urban environment, a satellite elevation of 45° and a mobile moving at 50km/h. The multipath channel is composed of a direct path having a rice factor of 7 dB, and 11 echoes with constant delay (from 46 to 316 ns) following Rayleigh distribution. The first two strongest echoes (relative power of -10dB with regard to the direct path) have a short delay of respectively 14 and 20 meters.

Simulations have been run with the following configuration: 2 minutes of signal with a sampling rate of 100MHz, 4ms integration time, early-late spacing set to 0.125 chip, 2nd order DLL with 1Hz bandwidth, 3rd order PLL bandwidth 5Hz aided by a 2nd order FLL bandwidth 5Hz. A number of C/No values have been considered from 25 to 55 dB-Hz step 5.

Choice of front-end filter Bandwidth

A number of filter front-end bandwidth have been tested. The first approach was to use the widest possible front-end filter in order to obtain the best tracking performances, consequently a 12MHz one sided filter was chosen to asses CBOC performances. In parallel the same simulations with a 8MHz one sided filter were performed. It surprisingly appears that the latter gave better results. After computation of the theoretical tracking error formulas it has been confirmed that for the chosen chip-spacing (0.125 chip) and integration time (4ms), the use of a filter with 8MHz one sided bandwidth provides better performances. Figure 5 presents the theoretical RMS code tracking error in function of the front end bandwidth.

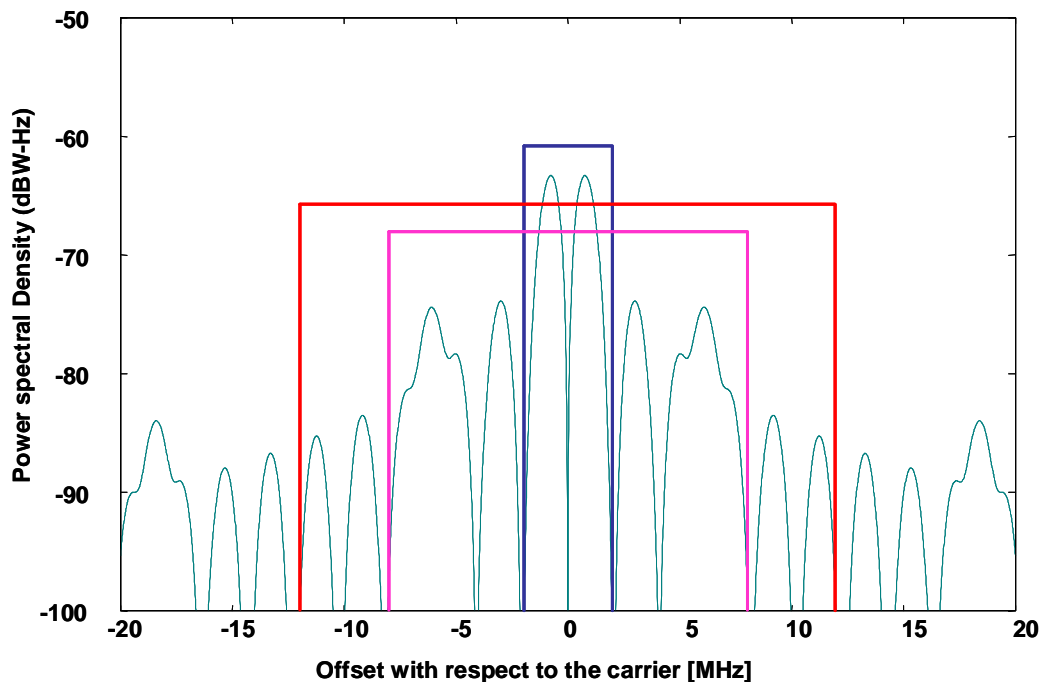


Fig. 4: Power spectral density of MBOC(6,1,1/11) and considered front-end filters bandwidths

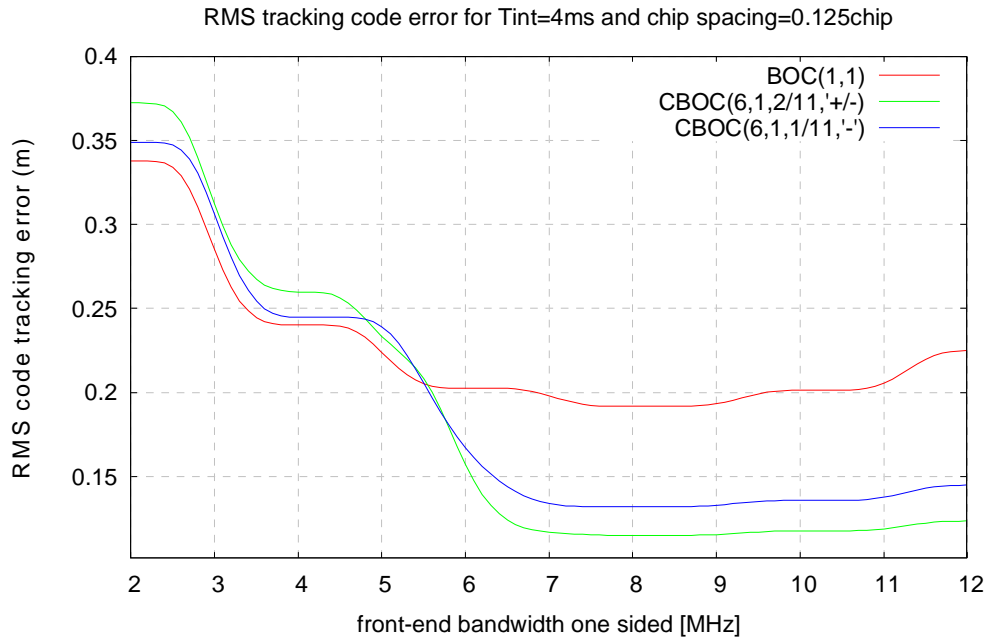


Fig. 5: RMS code tracking error in function of front-end bandwidth

Comparison CBOC/TM61/BOC11

Figure 6 presents the RMS code tracking error in white Gaussian noise for the BOC(1,1) baseline signal and CBOC signal received by a CBOC receiver, a TM61 receiver a BOC(1,1) receiver, for a front-end filter with 8MHz bandwidth one sided.

The best performance is obtained for a pure CBOC receiver receiving CBOC(6,1,2/11,+/-) where the pilot channel has a BOC(6,1) component with alternating sign; the corresponding TM61 receiver performs quite good with a degradation of 0.7 dB. Pure CBOC receiver receiving CBOC(6,1,1/11,-) on pilot channel performs 1.4 dB worth than CBOC(6,1,2/11,+/-) signal, and the corresponding TM61 receiver has a degradation of 0.6 dB. Compared to the Galileo baseline BOC(1,1), CBOC(6,1,2/11,+/-) provides an improvement of 5 dB for pure CBOC receiver, 4.3 dB for TM61 receiver but has a degradation of 0.7 dB when received by a BOC(1,1) receiver. Concerning CBOC(6,1,1/11,-) signal it provides an improvement of 3.5 dB for CBOC receiver, 2.9 dB for TM61 receiver and it has similar performances as the BOC(1,1) baseline signal when received by a BOC(1,1) receiver.

RMS code tracking Error
front-end filter bandwidth 8MHz one sided

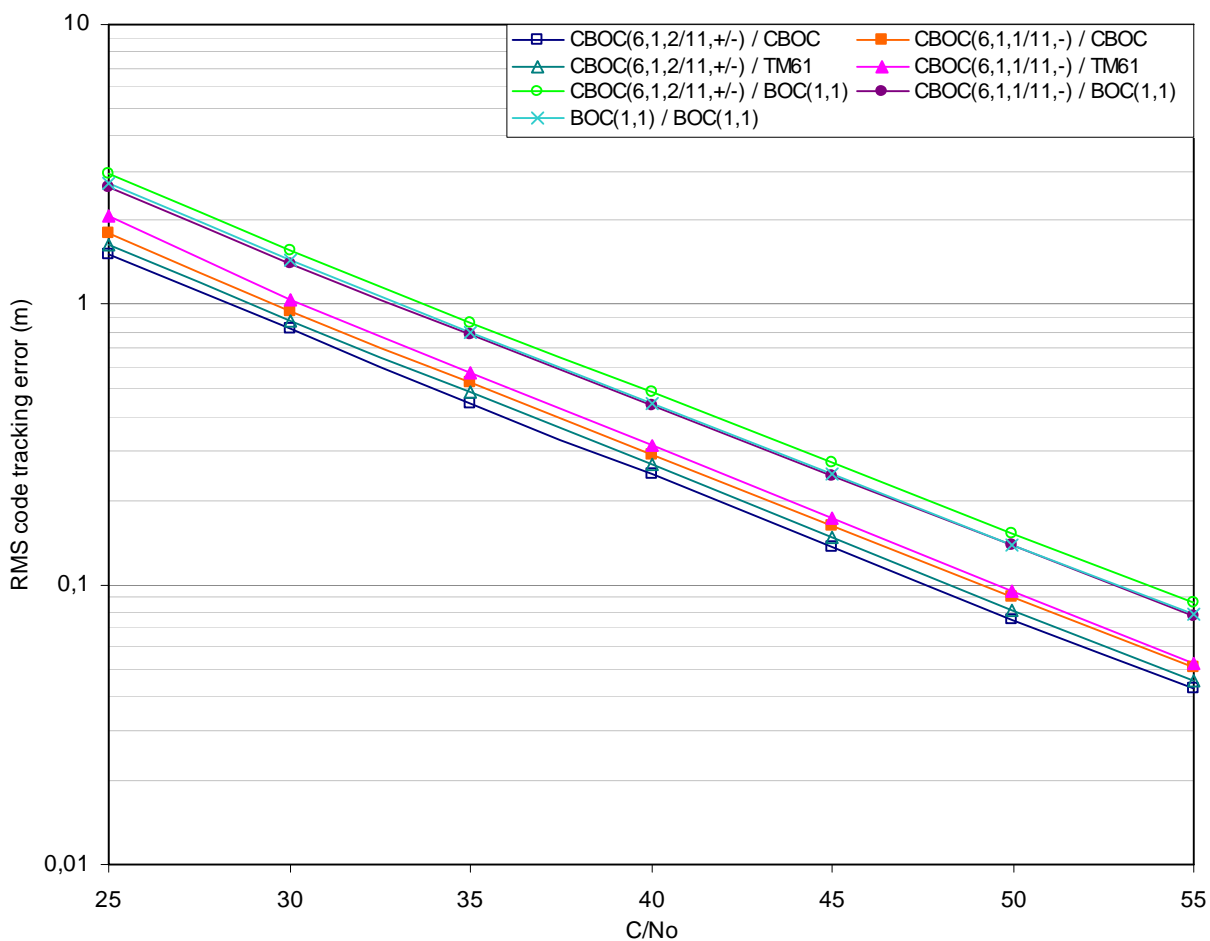


Fig 6: RMS code tracking error in meter for BOC(1,1) signal and CBOC signal received by a CBOC receiver, a TM61 receiver a BOC(1,1) receiver, front-end filter bandwidth 8MHz one sided

RMS code tracking Error in presence of multipath front-end filter bandwidth 8MHz one sided

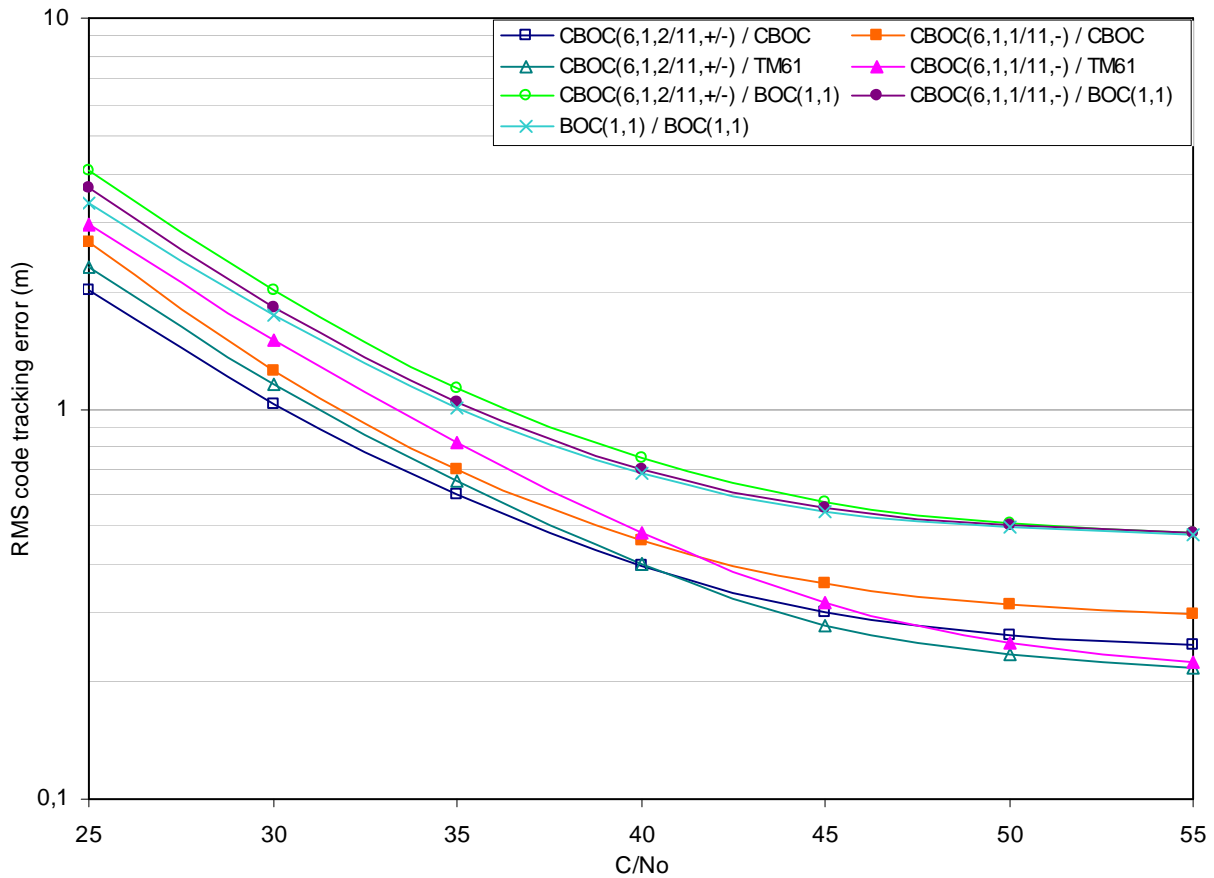


Fig 7: RMS code tracking error in meter for BOC(1,1) signal and CBOC signal received by a CBOC receiver, a TM61 receiver a BOC(1,1) receiver, front-end filter bandwidth 8MHz one sided, urban multipath environment

Figure 7 presents the RMS code tracking error for the same signals in white Gaussian noise and affected by multipath and Figure 8 presents the mean code tracking error due to multipath.

TM61 receivers that use pure BOC(6,1) for early-late correlation outperform pure CBOC receivers in terms of multipath resistance. Fig 6 shows that when C/No increases and multipath errors become predominant TM61 performs better than CBOC receiver in terms of RMS tracking error.

Mean code tracking Error in presence of multipath front-end filter bandwidth 8MHz one sided

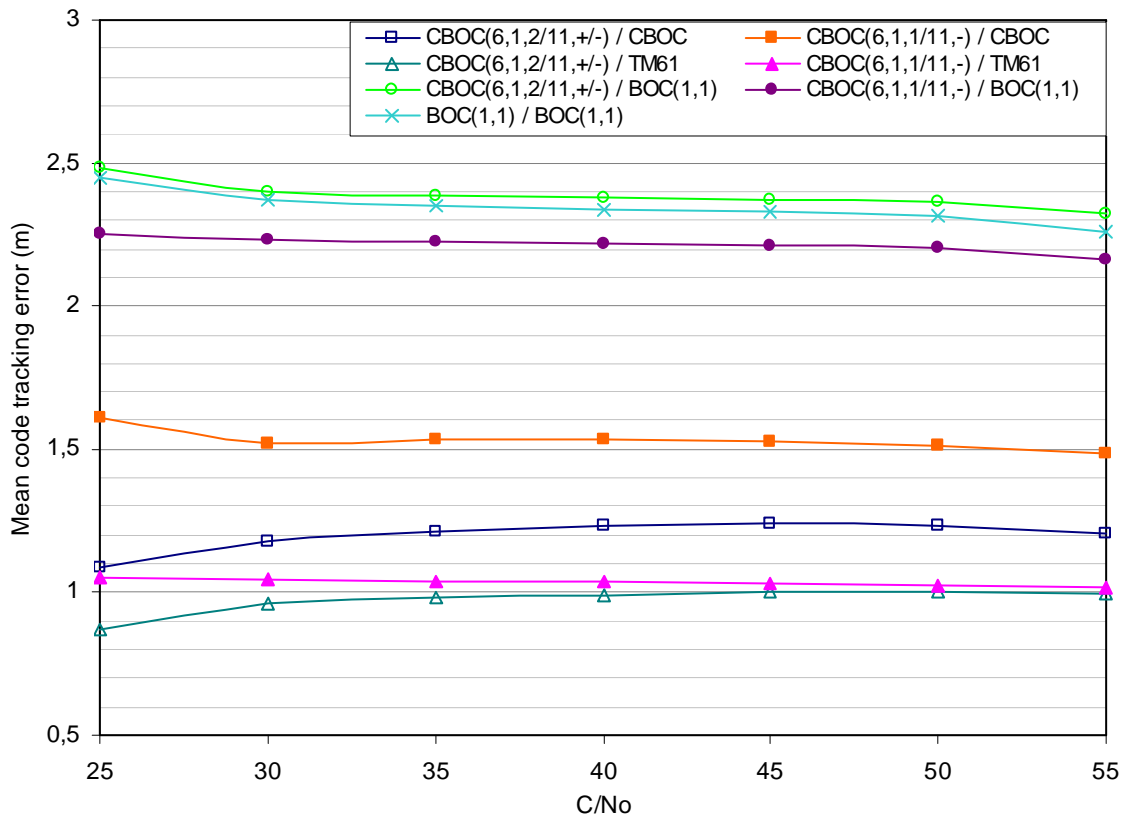


Fig 8: Mean code tracking error in meter for BOC(1,1) signal and CBOC signal received by a CBOC receiver, a TM61 receiver a BOC(1,1) receiver, front-end filter bandwidth 8MHz one sided, in urban multipath environment

BOC(1,1) receiver

It is proposed here to evaluate the compliance of the optimized signal CBOC with regards to receiver using only BOC(1,1). This type of receivers use a narrow input bandwidth, the minimum required bandwidth being 2MHz one sided.

Results are presented in figure 9. It is represented on the same figure the RMS code tracking error in thermal noise and in presence of mutipath, and the mean code tracking error in multipath for CBOC signal received by BOC(1,1) receiver and BOC(1,1) signal received by BOC(1,1) receiver.

Compared to the Galileo baseline BOC(1,1), in presence of thermal noise only, CBOC(6,1,1/11,-) signal received by BOC(1,1) receiver exhibits a 0.4dB degradation and CBOC(6,1,2/11,+/-) signal received by BOC(1,1) receiver 0.8 dB degradation. The resistance to multipath appears to be similar: the mean code tracking error is of the same order and the RMS tracking error tends to the same values for the three simulated signals when C/No increases.

**RMS and mean code tracking Error in presence of multipath
front-end filter bandwidth 2MHz one sided**

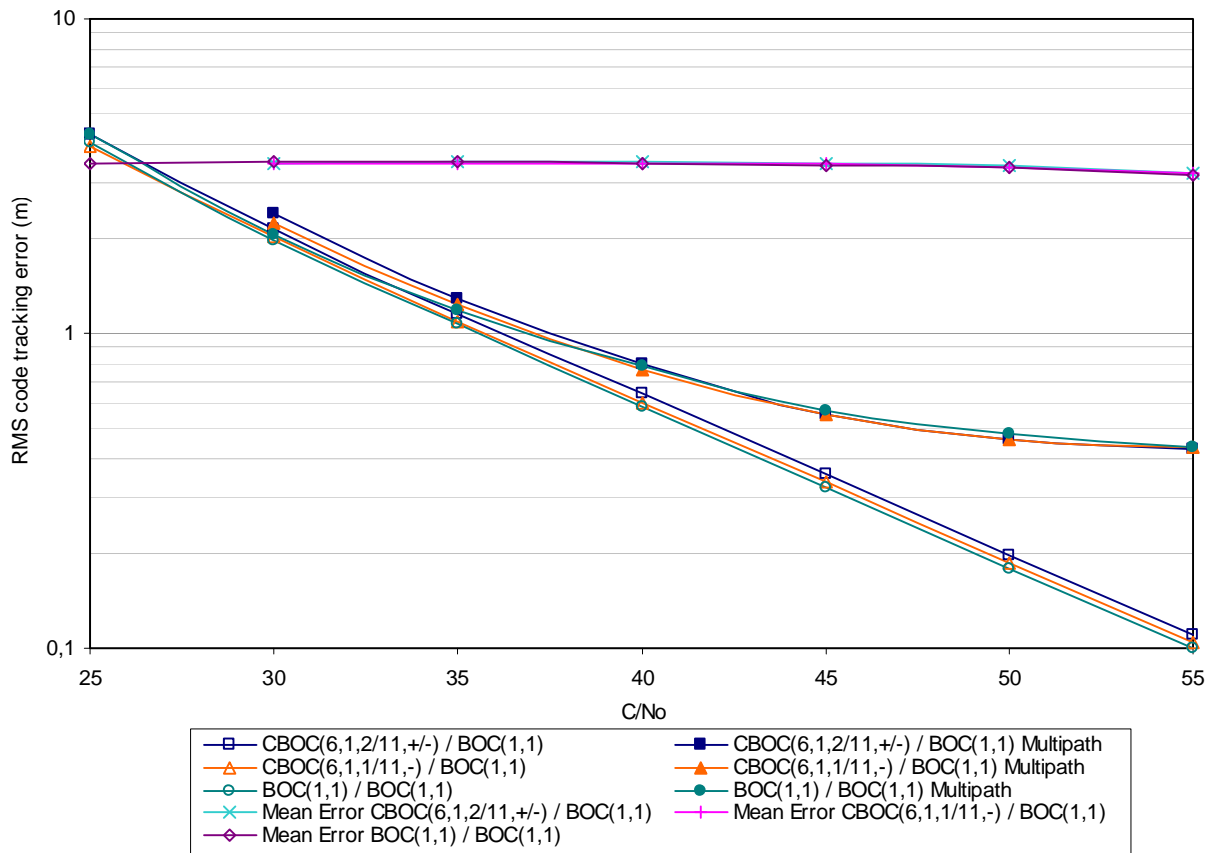


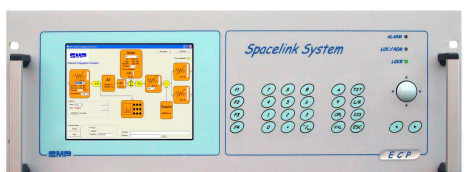
Fig 9: RMS code tracking error in meter for BOC(1,1) signal and CBOC signal received by BOC(1,1) receiver, front-end filter bandwidth 2MHz one sided, in thermal noise and urban multipath environment

RF EQUIPMENTS

After theoretical analysis and simulations, the following step would be to assess performances using real RF signals. CNES has made develop a number of equipments that should allow the generation of CBOC signal. It includes a flexible RF generator and a propagation channel emulator. The RF signal can then be digitalized and recorded using CNES’s broadband digitizer and high capacity recorder, and finally be post processed using the Juzzle software receiver.



Flexible signal generator



Propagation channel emulator



Broadband digitizer



High capacity data recorder

Fig. 10: laboratory’s RF equipments

Due to lack of availability of some of the laboratory equipments, the results can’t have been obtained on time and presented here. This will be done in further publication.

CONCUSION AND FUTURE WORK

The results obtained by simulations confirm the theoretical analysis: the proposed CBOC signal for the optimized Galileo L1 OS signal bring a significant improvement compared to tracking of a pure BOC(1,1) modulation. It remains true even for simplified receiver architecture such as the TM61 receiver, which provides a decrease in receiver complexity and keep a significant tracking improvement compared to pure BOC(1,1) signal, especially in terms of multipath resistance. Moreover CBOC signal prove to be compatible with simple BOC(1,1) receiver, the degradation introduced remains small.

Future work consists in continuing signal performance assessment using RF signal in order to get closer to real conditions.

REFERENCES

- [1] Hein G.W., Avila-Rodriguez J.-A., Wallner S., Pratt A.R., Owen J.I.R., Issler J.-L., Betz J.W., Hegarty C.J., Lt Lenahan L.S., Rushanan J.J.,Kraay A.L., Stansell T.A., "MBOC: The New Optimized Spreading Modulation Recommended for GALILEO L1 OS and GPS L1C", Proceedings of IEEE/ION PLANS 2006 –24-27 April 2006, San Diego, California, USA.
- [2] Avila-Rodriguez J.A., Wallner S., Hein G.W.,Rebeyrol E., Julien O., Macabiau C., Ries L., DeLatour A., Lestarquit L., Issler J.-L., "CBOC – An Implementation of MBOC", First CNES Workshop on Galileo Signals and Signal Processing , 12-13 October 2006, IAS (Institut Aero Spatial) Toulouse, France.
- [3] Julien O., Macabiau C., Ries L., Issler J.-L., "1-Bit Processing of Composite BOC (CBOC) Signals and Extension to Time-Multiplexed BOC (TMBOC) Signals", ION GNSS January 2007.
- [4] Julien, O., "Design of Galileo L1F Receiver Tracking Loops", *Ph.D. thesis, Department of Geomatics Engineering, University of Calgary, UCGE Report 20227.*
- [5] J. W. Betz, "The Offset Carrier Modulation for GPS modernization", in Proc. Of ION Technical meeting, pp. 639-648, 1999.